ELSEVIER

European Polymer Journal 39 (2003) 33–42

EUROPEAN POLYMER JOURNAL

www.elsevier.com/locate/europolj

Structural deviations in poly(amidoamine) dendrimers: a MALDI-TOF MS analysis

J. Peterson [a], V. Allikmaa [a], J. Subbi [b], T. Pehk [b], M. Lopp [c,*]

[a] *Institute of Chemistry at Tallinn Technical University, Akadeemia tee 15, 12618 Tallinn, Estonia*
[b] *National Institute of Chemical and Biological Physics, Akadeemia tee 23, 12618 Tallinn, Estonia*
[c] *Tallinn Technical University, Faculty of Chemistry, Ehitajate tee 5, 19086 Tallinn, Estonia*

Received 17 April 2002; received in revised form 10 June 2002; accepted 24 June 2002

Abstract

A step-by-step synthesis/purification (CC, HILIC, HPLC) of poly(amidoamine) PAMAM dendrimers was performed. MALDI-TOF MS in the linear and reflectron mode was used to analyze the purified samples and byproduct samples of G0–G5 generations of the dendrimers up to the mass of 35 000 Da. DHB/fucose was found to give the best resolution, causing the least fragmentation of the samples. The precise mass number for the ideally branched dendrimers and their "structural errors" was obtained. The profile of the structural errors was established.

Keywords: PAMAM dendrimers; MALDI-TOF MS; Structure deviations of PAMAM dendrimers

1. Introduction

Poly(amidoamine) (PAMAM) dendrimers are synthetic polymers with unique structural and physical characteristics. These dendrimers consist of an ethylenediamine (EDA) or ammonia initiator core, a repeating monomer unit of polyamidoamine ($-CH_2CH_2CONH-CH_2CH_2N<$) and a terminal amino group, which can be subsequently used in the synthesis of further generations of the dendrimer (Fig. 1).

Recent years have seen increased interest in characterizing the structure of PAMAM dendrimers. Several analytical techniques, including size exclusion chromatography (SEC) [1,2], low angle laser light scattering (LALLS) [2,3], infrared (IR) spectroscopy [4], capillary electrophoresis (CE) [5–7], MS (chemical ionization and fast-atom bombardment [8], laser desorption and electrospray ionization [9] and MALDI-TOF [10]) and ^1H, ^2H, ^{13}C NMR [1,4,8,11], were applied in these descriptions. Unfortunately, the performance of all these techniques declines with an increasing molecular weight.

This study focuses on the structural deviations in PAMAM dendrimers by stepwise synthesis of the EDA initiator-core PAMAM dendrimer with an amidoamine-repeating unit up to generation 5, using different chromatographic purification techniques, followed by simultaneous investigation of the MALDI-TOF MS spectra of the obtained fractions.

2. Experimental

2.1. Materials

The used matrixes 2,5-dihydroxybenzoic acid (DHB), 4-hydroxy-3-methoxycinnamic (ferulic acid), α-cyano-4-hydroxycinnamic acid, 1,8,9-anthracenetriol (dithranol), and D-(+)-fucose were obtained from Aldrich and used without further purification. Substance P, insulin β-chain, bovine insulin and horse heart cytochrome C were purchased from Sigma.

* Corresponding author. Tel.: +372-6204366; fax: +372-6547520.
E-mail address: lopp@chemnet.ee (M. Lopp).

0014-3057/02/$ - see front matter
PII: S0014-3057(02)00188-X

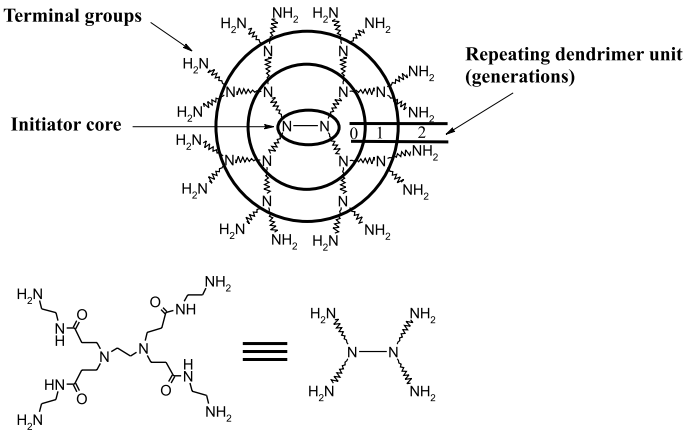

Fig. 1. Schematic diagram of a polyamidoamine dendrimer. The compound is a second-generation dendrimer.

2.2. Preparation and chromatographic purification of PAMAM dendrimers

The construction of an EDA-core PAMAM dendrimer consist of two consecutive steps: Michael addition of primary amine (EDA in the very first step) to methyl acrylate followed by amidation of the formed multiester (tetraester at the very beginning) with EDA (Fig. 2) [1,2,8].

The first six generations (generations 0–5) of EDA-core polyamidoamine dendrimers were synthesized in the stepwise process described in [6]. In order to obtain less complicated MS spectra (minimize both the intramolecular defects, missing repeating units, intramolecular loops) and intermolecular aggregates (dimers) as well as lower generation dendrimers, different chromatographic purification procedures of the multiester compounds G0.5–G4.5 were used. The generations −0.5, 0.5 and 1.5 were purified by column chromatography on a silica gel; G2.5, G3.5, and G4.5 by column chromatography on Sephadex LH-20. In both cases, methanol or its mixture with dichloromethane was used as the eluent. The generation homogeneity of the synthesized dendrimers was followed by capillary zone electrophoresis (CZE) [6,7] and by ^{1}H and ^{13}C NMR spectroscopy.

The first full generation dendrimer (G1) was purified using hydrophilic interaction chromatography (HILIC) and high-pressure liquid chromatography (HPLC).

HILIC. 10 × 150 mm glass column was filled with 55 mg Silasorb Diol (10 μm; Chemapol Prague, Czechoslovakia). 1 mg G1 was dissolved in 100 μl acetonitrile/water (1:1) mixture and inserted into the column. Air pressure (0.1 bar) was applied to the column, and the first fraction was collected. The next fractions were

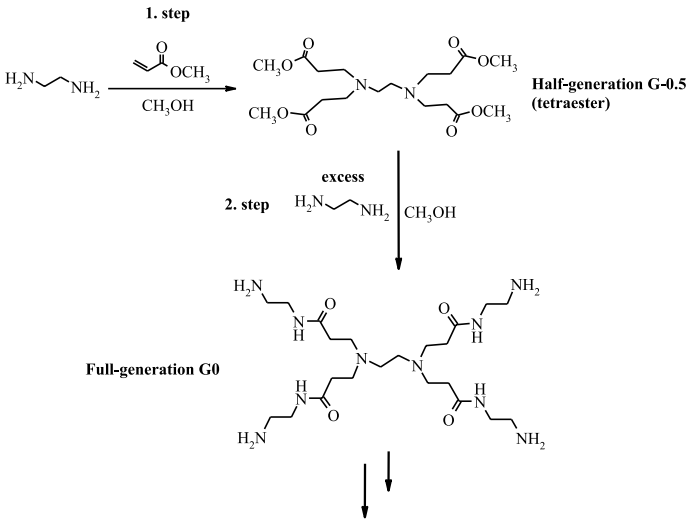

Fig. 2. Diagram of the synthesis of EDA-core PAMAM dendrimers.

Table 1
^{13}C and ^{1}H NMR chemical shifts in the first generations of EDA-core PAMAM dendrimers in the $CDCl_3$ solution

Group	No. of C	^{13}C G0.5	^{1}H	^{13}C G0	^{1}H	^{13}C G0.5	^{1}H	^{13}C G1	^{1}H	^{13}C G1.5	^{1}H	^{13}C G2	^{1}H	^{13}C G2.5
$-C^*H_2N<$	2	52.17	2.47	51.89	2.42	51.15	2.55	51.03	2.46	50.84	2.55	50.84	2.47	50.44
NCH_2^*	4	49.68	2.74	50.49	2.67	50.03	2.77	49.84	2.67	49.84	2.76	49.84	2.68	49.60
C^*H_2CO	4	32.54	2.42	34.27	2.36	33.69	2.36	33.53	2.26	33.37	2.36	33.38	2.35	33.39
C^*OO	4	172.89	–	–	–	–	–	–	–	–	–	–	–	–
$COOC^*H_3$	4	51.46	3.65	–	–	–	–	–	–	–	–	–	–	–
C^*ONH^*	4			173.11	7.69	172.18	7.19	172.55	8.1	172.16	7.78	172.37	7.80	172.20
NHC^*H_2	4			42.26	3.27	37.05	3.28	37.63	3.16	37.23	3.27	37.36	3.23	37.03
$C^*H_2N<$	4			41.48	2.80	52.82	2.55	52.64	2.47	52.18	2.59	52.21	2,48	51.81
$>NC^*H_2$	8					49.15	2.77	50.37	2.69	49.62	2.81	49.84	2.69	49.50
C^*H_2CO	8					32.54	2.44	34.09	2.3	33.51	2.37	33.67	2.30	33.39
C^*OO	8					172.87	–	–	–	–	–	–	–	–
$COOC^*H_3$	8					51.49	3.72	–	–	–	–	–	–	–
C^*ONH^*	8							172.90	7.89	172.05	7.05	172.42	7.98	171.88
NHC^*H_2	8							42.11	3.22	36.91	3.28	37.44	3.23	36.94
$C^*H_2N<$	8							41.37	2.75	52.63	2.55	52.53	2.46	51.92
$>NC^*H_2$	16									48.97	2.76	50.16	2.67	49.32
C^*H_2CO	16									32.4	2.44	33.91	2.29	33.26
C^*OO	16									172.76	–	–	–	–
$COOC^*H_3$	16									51.35	3.67	–	–	-
C^*ONH^*	16											172.82	7.89	171.80
NHC^*H_2	16											42.01	3.22	36.65
$C^*H_2N<$	16											41.25	2.75	52.35
$>NC^*H_2$	32													48.72
C^*H_2CO	32													32.14
C^*OO	32													172.45
$COOC^*H_3$	32													51.04

collected analogously, using 100 μl of the same eluent, 2×100 μl of distilled water, 2×100 μl of distilled water acidified with acetic acid to pH = 3.39, and finally, with 2×100 μl of distilled water/acetic acid (pH = 2.98). The resulting fractions were lyophilized and analyzed by MALDI-TOF MS.

HPLC. HPLC analysis was carried out on the Shimadzu system: LC 10AT vp HPLC pump, SPD-10A VP UV–VIS detector and SCL-10A VP system controller. The date was collected and analyzed on a Shimadzu ClassVP software. Samples of G1 (40 μl, $c = 8$ mg/ml) were analyzed in a Symmetry C_{18} column (4.6×250 nm, 5 μm), detection at 218 nm. The eluent system was (A) 0.1% trifluoroacetic acid in water, (B) acetonitrile. The linear gradient 0–50% of B in 20 min was used (1 ml/min). The different fractions were collected, lyophilized, and analyzed by MALDI-TOF MS.

2.3. NMR spectrometry

The structure of lower generation dendrimers was confirmed by ^{1}H and ^{13}C NMR high field (11.7 T) spectroscopy on an AMX500 MHz Bruker instrument. The samples were dissolved and measured in the $CDCl_3$ solution. In the case of higher generations, a small amount of CD_3OD was added to improve their solubility (additional effects on the C-13 spectra do not exceed 0.2 ppm). 2D FT ^{1}H–^{13}C COSY correlation diagrams were applied to resolve the overlapping of ^{1}H signals. The ^{1}H and ^{13}C NMR chemical shifts in the first generations of EDA-core PAMAM dendrimers are presented in Table 1. The assignments slightly differ from those presented in [8].

2.4. MALDI-TOF mass spectrometry

A dendrimer solution was prepared by dissolving 1 mg of the purified dendrimer syrup in 1 ml of water. Additionally, a 1:10 dilution of this solution was made. The matrix solution was prepared by dissolving 10 mg of matrix in 1 ml of the 1:1 mixture of the deionized water and acetonitrile. The analytical sample was prepared by mixing the dendrimer solution (1 μl) with the matrix solution (1 μl) on a stainless steel probe tip, and this mixture was allowed to dry at room temperature.

The MALDI mass spectra were recorded on two different time-of-flight MALDI mass spectrometers (both original equipment built at the National Institute of Chemical Physics and Biophysics, Estonia). In the case of lower dendrimer generations, the instrument with a reflectron mode and with a delayed extraction was used.

For a higher dendrimer generations, the instrument with linear delayed extraction MALDI technique was used.

In the reflectron mode, a 2.6 kV pulsed extraction and a 14.6 kV total acceleration voltage were applied. The delay was optimized separately for different mass ranges. A double multichannel plate detector with a conversion dynode was used for ion detection and a Tektronics TDS 520 digitizing oscilloscope, for data accumulation. An excimer laser pumped dye laser working at 340 nm was used for desorption/ionization.

The other mass spectrometer that was used in linear mode, was equipped with an ETP AF850H electron multiplier with a conversion dynode as the detector and an XeF excimer laser at the wavelength of 351 nm for desorption. For mass calibration in different mass ranges, standard compounds such as substance P, insulin β-chain, bovine insulin and horse heart cytochrome C, were used.

Different standard MALDI matrixes such as 2,5-dihydroxybenzoic acid, 4-hydroxy-3-methoxycinnamic acid, α-cyano-4-hydroxycinnamic acid, dithranol and DHB/fucose (1:1 mixture) were used.

3. Results and discussion

3.1. MALDI-TOF MS analysis of the synthetic fractions

Of all mass spectrometric methods MALDI-TOF MS is most tolerant to impurities. It produces predominantly single charged ions, allowing for the determination of the direct mass number of oligomers, which can produce true molecular weight distributions for the narrow-distributed polymers. However, in polymers with wide mass distributions or blends of polymers, different mass dependent or oligomer-specific discrimination effects appear, and quantitative conclusions can be drawn only by involving other analytical methods as well [12].

Up to generation G1.5, the spectra near MALDI threshold consist of sharp lines corresponding to ideally branched and defective protonated dendrimers, their fragmentation products, and weak lines corresponding to Na and K adducts. Starting from G2.5, unresolved background signals emerge. Already for G4.5, the spectra line structure was lost. Still, the mean molecular weight distribution was readily observed.

The full generations of PAMAM dendrimers have numerous amino groups with good proton accepting ability in the outer shell and can readily be ionized by proton addition. In higher generations, the spectral lines became weak and, as a result, excessive laser power was needed. The best spectra for both a half and full generations signal were obtained when a 1:1 DHB/fucose mixture, a well-known "cold" matrix, was used [13,14]. However, it also caused a background to emerge beginning from G2, probably due to the trapping of the sugar molecules inside the dendrimer framework.

MALDI mass spectra for all half and full generations of the dendrimer up to G5 in the linear mode and up to G2.5 in the reflectron mode gave direct information about the possible "structural errors". The full isotopic resolution and superior mass accuracy of the reflectron mode was used to confirm our assignments of the defective dendrimer structures and prompt decay products. For generations G4 and G5, we did not obtain a line structure in the MS spectra (Fig. 3). Still, a general molecular weight distribution was well observed. Un-

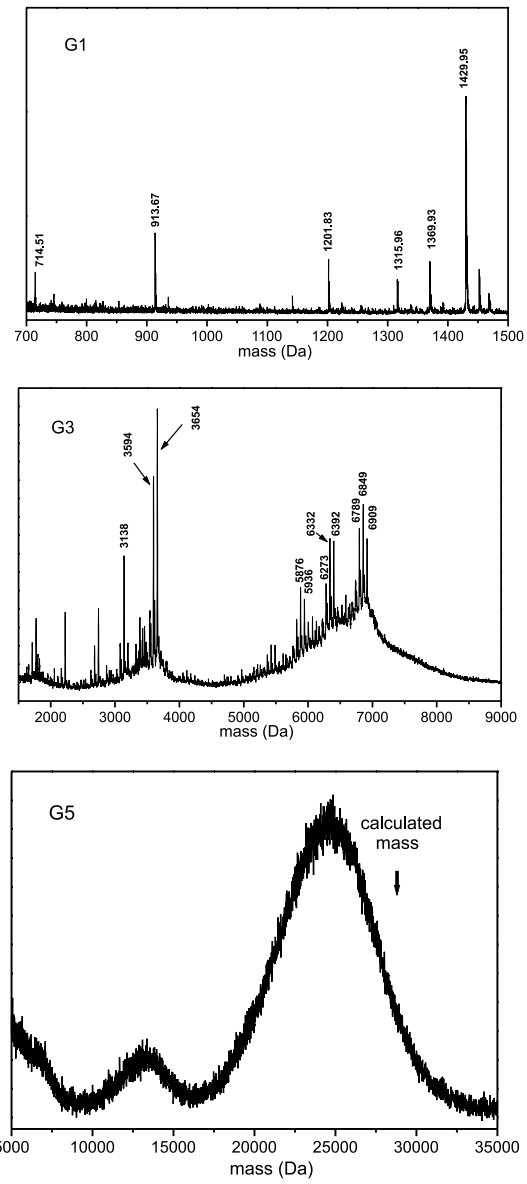

Fig. 3. MALDI-TOF MS spectra for the first, third and fifth PAMAM generations.

fortunately, the MALDI-TOF method does not provide for the straightforward quantification of the sample investigated. Therefore we did not obtain the "real" generation distribution. However, discrimination is generally against the higher mass, so it can lead only to overestimation of the lower mass impurities. Despite the above limitations we have matched all lines in the spectra with the corresponding structures of structural errors (Fig. 4).

Mass numbers exceeding the mass of an ideally branched dendrimer by +22 and +38 are the corresponding Na and K salts (ionization by Na and K are due to random Na and K impurities in the samples). The calculated mass numbers of the structural errors are in very good agreement with those derived from the spectra (Table 2).

The fragmentation of an analytical sample can lower the intensity, causing sharp lines to emerger due to a prompt decay inside the ion source. These secondary lines may interfere with the interpretation of the parent lines from the primary structural error lines of dendrimers. These secondary lines can be excluded through matrix and laser intensity dependencies and from the possible mass numbers of the non-fragmented molecular ions. To elucidate the fragmentation of PAMAM dendrimers during the MALDI analysis in the linear mode and to differentiate those from the parent lines of the primary lines, the laser intensity was varied up to twofold from threshold for G1, G1.5 and G2 using different matrixes. As a rule, with higher laser intensity the lines were widened up to the loss of line structure and a weakly structured background emerged. The

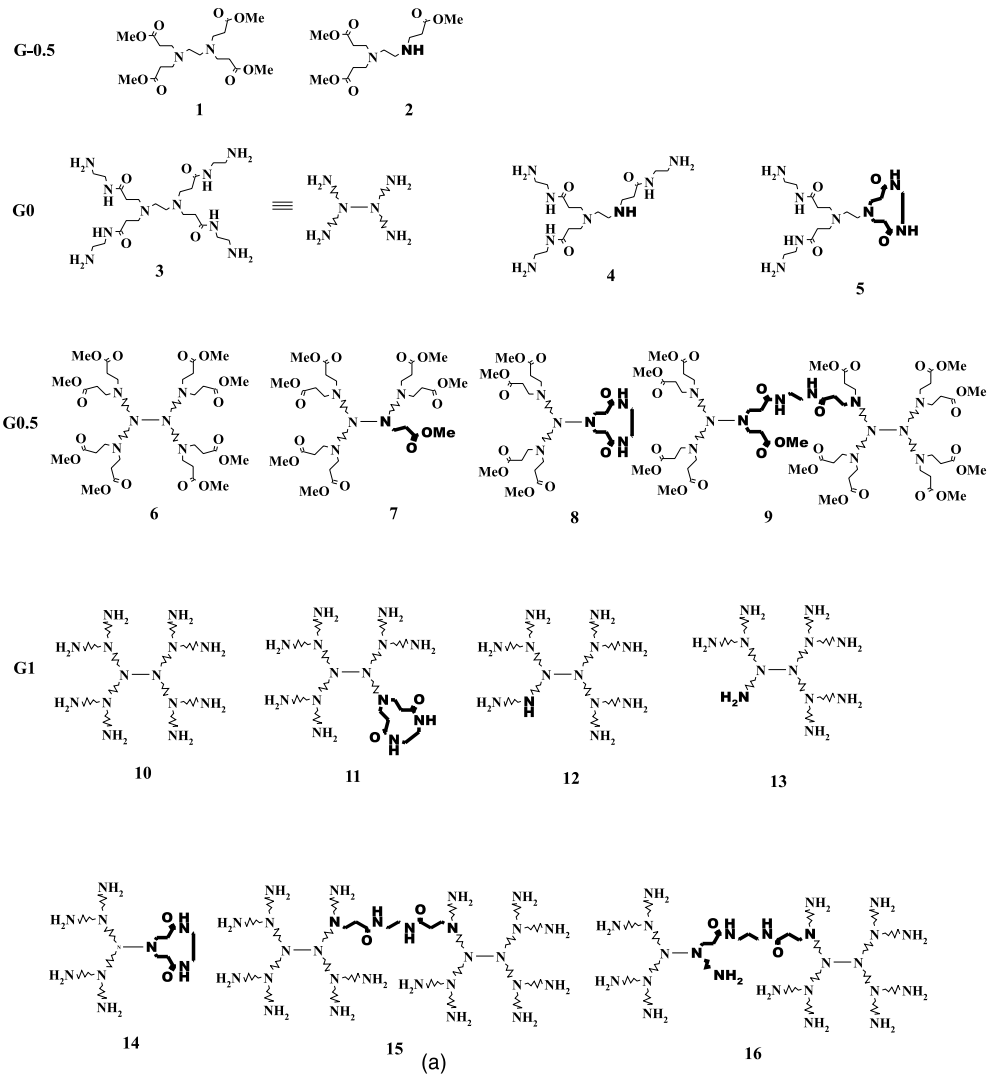

Fig. 4. PAMAM dendrimer structures detected through MALDI-TOF MS.

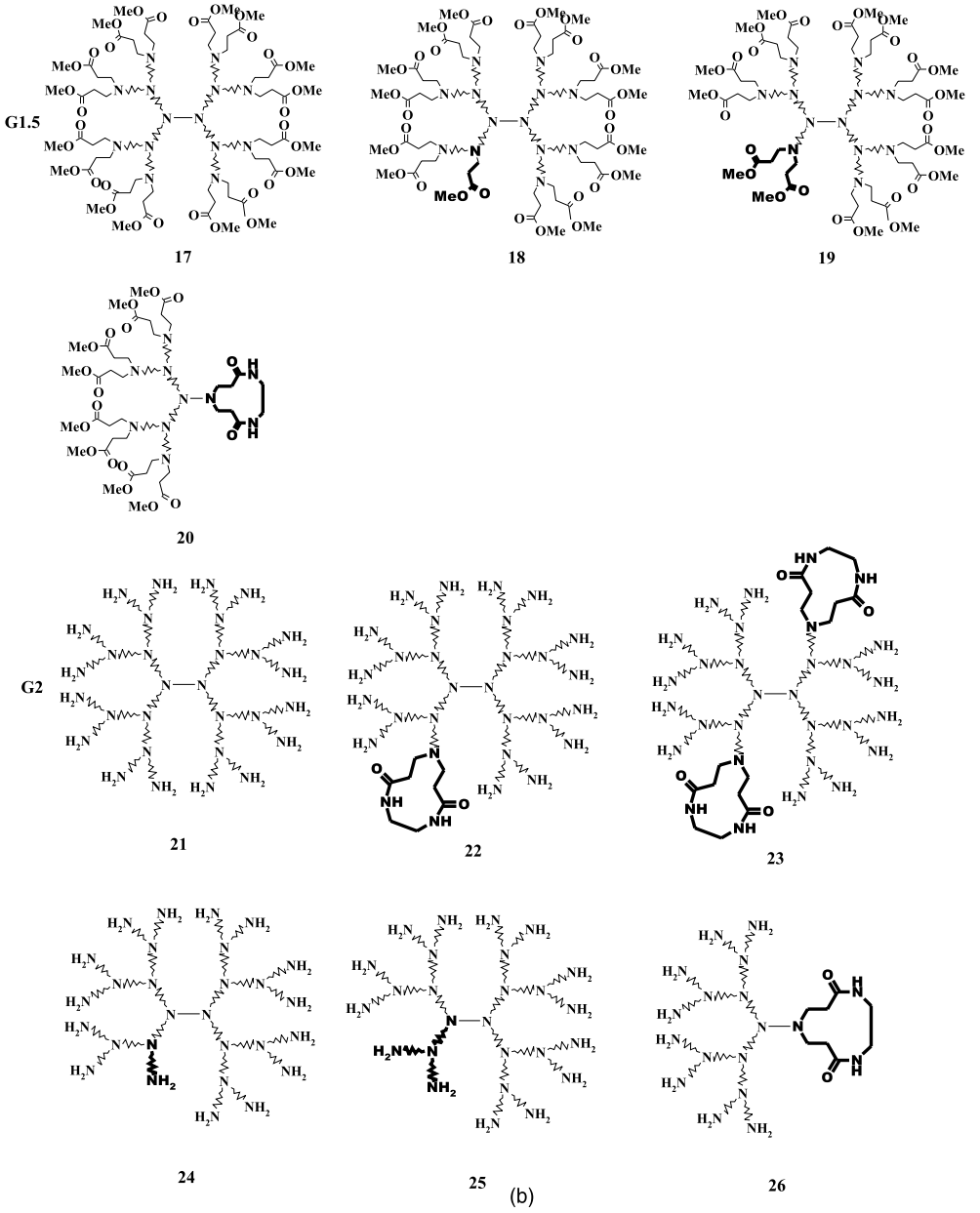

Fig. 4 (*continued*)

DHB/fucose matrix again provided the best signal and caused the least fragmentation of the dendrimer. Our experiments also proved α-cyano-4-hydroxycinnamic acid to be a ''hot'' matrix, causing most of the fragmentation, similar to the case of peptides and proteins [15,16]. DHB and ferulic acid lie between these two in this respect.

In all spectra from G0.5 to G2 (Fig. 3), we observed a line exactly at half the dendrimer mass visible even at the threshold intensity. The isotope structure of this line indicates that it corresponds to a single charged ion (the appearance of multiply charged ions in MALDI MS is strongly suppressed; also, no ions at mass (M+2H)/2 appear). As no protonated ion with such mass can exist, we identified the line as a dendrimer fragmentation product, where the central C–C bond in the EDA-core is broken. The negatively charged part of the molecule is neutralized by a proton, leaving a positive ion with half the dendrimer mass (Fig. 5). The corresponding fragmentation of ethylenediamine derivatives is known also from the MS spectra [17]. The half-mass line could be

Table 2
Mass numbers determined for ideally branched and defective PAMAM dendrimers from the MALDI MS spectra

Generation	Experimentally determined molecular mass	Calculated molecular mass	Number of compounds in Fig. 4
−0.5	405.11	405.22	1
	319.08	319.18	2
	202.05	202.11	$(1/2M)^+$
0	517.35	517.39	3
	403.26	403.31	4
	457.28	457.32	5
	258.13	258.19	$(1/2M)^+$
0.5	1205.52	1205.68	6
	1005.47	1005.56	7
	801.41	801.46	8
	602.27	602.34	$(1/2M)^+$
	2008.14	2008.38	9
1	1429.95	1430.02	10
	1369.93	1369.95	11
	1315.96	1315.94	12
	1201.83	1201.86	13
	913.67	913.63	14
	714.51	714.51	$(1/2M)^+$
	2800.30	2800.66	15
	2343.50	2343.06	16
1.5	2806.25	2806.61	17
	2606.10	2606.49	18
	2405.98	2406.37	19
	1601.65	1601.93	20
	1402.56	1402.80	$(1/2M)^+$
2	3257.1	3257.2	21
	3196.9	3197.1	22
	3136.8	3137.0	23
	3028.6	3028.9	24
	2800.3	2800.6	25
	1827.3	1827.4	26
	1627.8	1628.1	$(1/2M)^+$

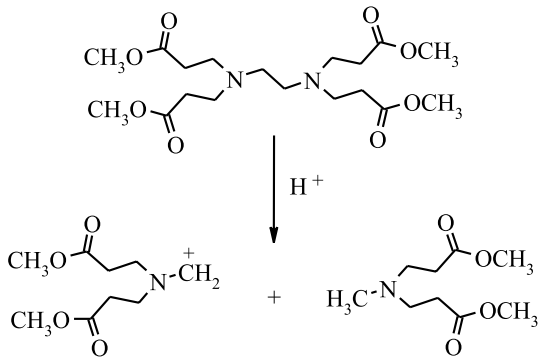

Fig. 5. Dendrimer formation with a mass half of that of an ideally branched dendrimer.

followed up to G3, with its intensity diminishing as compared to total intensity, with the growth of the dendrimer, especially in full generations.

3.2. PAMAM dendrimer structural errors profile

The structures of the structural errors of PAMAM dendrimers were described and characterized in [1,2,8–10,18]. The PAMAM structural errors can be divided into two main groups: "errors" that occur in the course of the synthesis and those from the destruction of the dendrimer. We have performed a systematic MALDI MS study of the purified PAMAM generations, separated minor impurities, confirmed the presence of some of the predicted "errors" and found some other deviated compounds. The typical spectra for the assignment of the structural error profile are presented in Fig. 6. The purification, the MALDI MS approach was especially fruitful for discovering minor higher molecular weight dendrimers (e.g. dimers), which were detects only after a special purification procedure that reduced the noise of

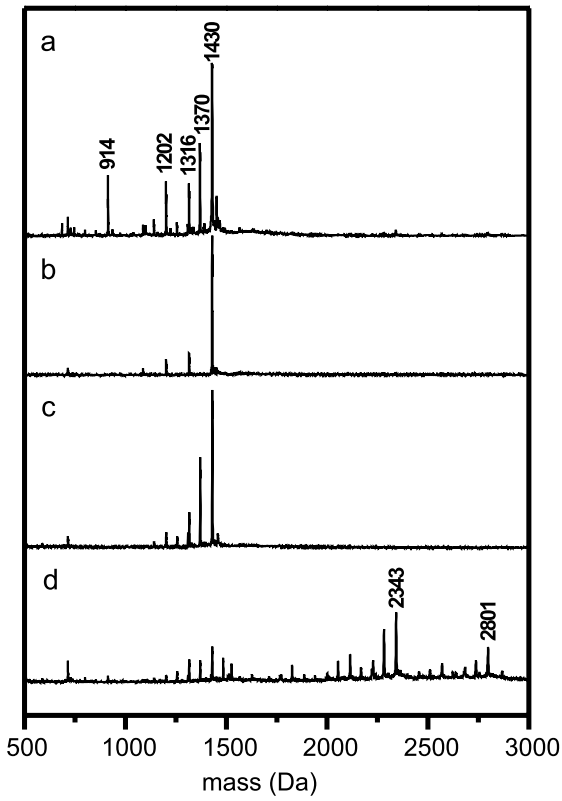

Fig. 6. MALDI-TOF MS spectra of G1. (a) G1 without purification; (b) purified by HILIC (defects 11 and 14 Fig. 4 are separated); (c) purified by HPLC (defect no. 14 is separated, the content of defects 12 and 13 is minimized); (d) the last fraction of HPLC purification, containing mainly dimers 15 and 16 and their "errors".

other structural units (Fig. 6d, Fig. 7, path c). The amount of separated structural errors—rich fractions was not sufficient for the NMR assignment of their structure.

HILIC separation that depends on the number of amino groups in the outer layer of the dendrimer allowed for the separation of the defects caused by intramolecular cyclization from the mixture of the first generation defective dendrimers (Fig. 4, compounds **11** and **14**, Fig. 6a, lines 1370 and 914). The HPLC method was suitable for the separation of some defects according to their molar mass. The lowest molar mass defect in the first generation is compound no. **14** (Fig. 4, Fig. 6a, line 914), which could be completely separated from the mixture. By using the HPLC, the content of "errors" (Fig. 4, compounds **12** and **13**, Fig. 6a, lines 1316 and 1202) also decreased markedly. Defective dendrimer no. **11** (Fig. 4, Fig. 6a, line 1370), having mass very close to that of G1 itself, could not be separated by this chromatographic method. The HPLC method also allowed the separation of the dendrimer "dimers" (Fig. 4, compounds **15** and **16**, Fig. 6d, lines 2801 and 2343), which could not be clearly identified by MALDI MS before chromatographic purification. The spectra in Fig. 6 convincingly prove that the defective dendrimers observed in the mass spectra of various generations of PAMAM dendrimers were formed in the course of the side reactions during the synthesis rather than during the fragmentation of an ideally branched dendrimer during the analysis. In the silica gel purified fractions (G0.5),

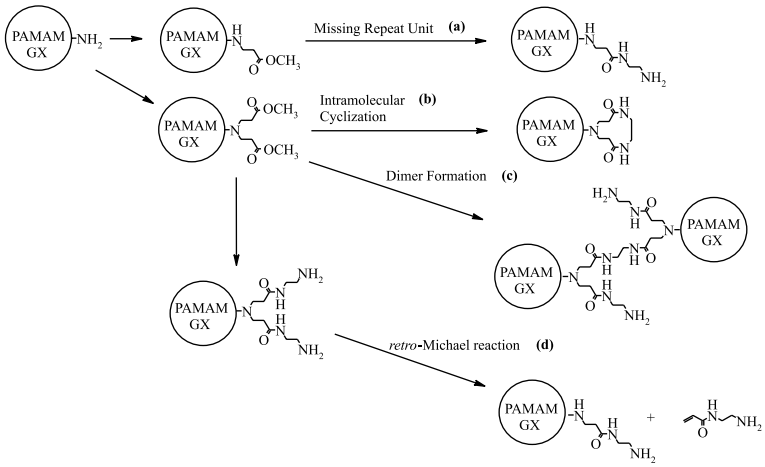

Fig. 7. Concurrent reactions in PAMAM dendrimer synthesis.

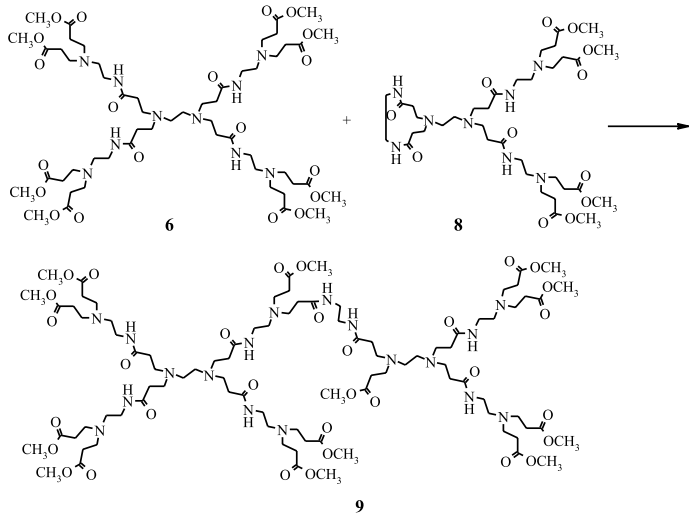

Fig. 8. Dimer formation during the synthesis of the half generation.

lines corresponding to the dimeric structure (Fig. 4, compound **9**) exist. This structure may form compounds G0.5 and "error" **8** (according to Fig. 8). This type of lines are also appears in higher generations. The quantity of the "ordinary" dimers (according to Fig. 7, path c) is quite small and the corresponding line is nearly on the level of noise. This kind of dimer (Fig. 4, compound **15**) can only be formed in the synthesis of a full generation.

The primary side reactions in the Starburst PAMAM dendrimer synthesis are those of the incomplete Michael addition, resulting in unsymmetrical dendrimeric structures (Fig. 7, path a). These products are clearly seen in the MALDI MS spectra of the PAMAM dendrimer early generations (Fig. 4, compounds **2**, **4**, **7**, **12**, **13**, **18**, **19**, **24**, **25**).

Additionally, the structural errors can form via intramolecular cyclization during the formation of a the full generation of the dendrimer (Fig. 7, path b; Fig. 4, compounds **5**, **8**, **11**, **14**, **20**, **22**, **23**, **26** detected by MALDI MS). The presence of many identical ester groups in the outer shell provides different cyclization possibilities. As a result, a wide variety of different types of cyclizized products is formed (e.g., Fig. 4, compounds **5** vs **11**; compounds **22** vs **23**, etc.).

One source of the structural errors is the retro-Michael reaction (Fig. 7, path d). We have recently shown that the Michael reaction is in equilibrium with its "retro" version [19]. This equilibrium depends strongly on temperature and is significant already in determining the structural deviations at room temperature. The detected compounds **2**, **4**, **12**, **13**, **24**, **25** (Fig. 4) may arise from both—the incomplete Michael reaction or the retro-Michael reaction, which allows us to complement the PAMAM dendrimer error formation scheme [18].

The results obtained from the MALDI-TOF spectra together with the data published about the CZE analysis of PAMAM dendrimers [5–7] and GC fragmentation data of the early generations of these dendrimers [19] are in good accordance with the chemical consideration of the formation of structural errors of the PAMAM dendrimer. A general conclusion, however, is that when choosing "cold" matrixes and working close to the threshold intensities, the MALDI method conveys important structural information for the PAMAM dendrimer lower generations and offers a tool for estimating the mass distribution for higher generations of the dendrimer.

Acknowledgement

The authors are grateful to the Estonian Science Foundation for the financial support (grants 5133, 3781, 4226).

References

[1] Smith PB, Martin SJ, Hall MJ, Tomalia DA. A characterization of the structure and synthetic reactions of polyamidoamine Starburst polymers. In: Mitchell Jr J, editor. Applied polymer analysis and characterization. München: Hanser; 1987. p. 357–85.

[2] Tomalia DA, Naylor AM, Goddard III WA. Starburst dendrimers: molecular-level control of size, shape surface chemistry, topology, and flexibility from atoms to macroscopic matter. Angew Chem Int Ed Engl 1990;29:138–75.

[3] Tomalia DA, Baker H, Dewald J, Hall M, Kallos G, Martin S, et al. Dendritic macromolecules: synthesis of starburst dendrimers. Macromolecules 1986;19(9):2466–8.

[4] Meltzer AD, Tirrell DA, Jones AA, Inglefield PT. Chain dynamics in poly(amidoamine) dendrimers. A study of ^{13}C NMR relaxation parameters. Macromolecules 1992;25(18):4541–8.

[5] Brothers II HM, Piehler LT, Tomalia DA. Slab-gel and capillary electrophoresis characterization of polyamidoamine dendrimers. J Chromatogr A 1998;814:233–46.

[6] Peterson J, Ebber A, Allikmaa V, Lopp M. Synthesis and CZE analysis of PAMAM dendrimers with an ethylenediamine core. Proc Estonian Acad Sci Chem 2001;50(3):156–66.

[7] Ebber A, Vaher M, Peterson J, Lopp M. Application of capillary zone electrophoresis to the separation and characterization of poly(amidoamine) dendrimers with an ethylenediamine core. J Chromatogr A 2002;949:351–8.

[8] Tomalia DA, Baker H, Dewald JR, Hall M, Kallos G, Martin S, et al. A new class of polymers: starburst-dendritic macromolecules. Polym J 1985;17:117–32.

[9] Kallos GJ, Tomalia DA, Hedstrand DM, Lewis S, Zhou J. Molecular weight determination of a polyamidoamine starburst polymer by electrospray ionization mass spectrometry. Rapid Commun Mass Spectrom 1991;5:383–6.

[10] Zhou L, Russell DH, Zhao M, Crooks RM. Characterization of poly(amidoamine) dendrimers and their complexes with Cu^{2+} by matrix-assisted laser desorption ionization mass spectrometry. Macromolecules 2001;34:3567–73.

[11] Meltzer AD, Tirrell DA, Jones AA, Inglefield PT. Chain dynamics in poly(amidoamine) dendrimers. A study of ^{2}H NMR relaxation parameters. Macromolecules 1992;25(18):4549–52.

[12] Nielen MWF. Maldi time-of-flight mass spectrometry of synthetic polymers. Mass Spectrom Rev 1999;18:309–44.

[13] Billeci TM, Stults JT. Tryptic mapping of recombinant proteins by matrix-assisted laser desorption/ionization mass spectrometry. Anal Chem 1993;65:1709–16.

[14] Gusev AI, Wilkinson WR, Proctor A, Hercules DM. Improvement of signal reproducibility and matrix/comatrix effects in MALDI analysis. Anal Chem 1995;67(6):1034–41.

[15] Karas M, Bahr U, Strupat K, Hillenkamp F, Tsrbopoulos A, Pramanik BN. Matrix dependence of metastable fragmentation of glycoproteins in MALDI TOF mass spectrometry. Anal Chem 1995;67(3):675–9.

[16] Kaufmann R, Chaurand P, Kirsch D, Spengler B. Post-source decay and delayed extraction in matrix-assisted

laser desorption/ionization-reflectron time-of-flight mass spectrometry. Are there trade-offs. Rapid Commun Mass Spectrom 1996;10:1199–208.

[17] Eight peak index of mass spectra. 2nd ed. vol 1. Aldermaston, England: Mass Spectrometry Data Centre; 1974.

[18] Tolić LP, Anderson GA, Smith RD, Brothers II HM, Spindler R, Tomalia DA. Electrospray ionization Fourier transform ion cyclotron resonance mass spectrometric characterization of high molecular mass Starburst™ dendrimers. Int J Mass Spectrom Ion Process 1997;165/166(II):405–18.

[19] Peterson J, Allikmaa V, Pehk T, Lopp M. Fragmentation of PAMAM dendrimers in methanol. Proc Estonian Acad Sci Chem 2001;50(3):167–72.